

Dynamic competition between transcription initiation and repression: Role of non-equilibrium steps in cell to cell heterogeneity

Namiko Mitarai,* Szabolcs Semsey, and Kim Sneppen†

Center for Models of Life, Niels Bohr Institute, University of Copenhagen, Blegdamsvej 17, 2100 Copenhagen, Denmark.

(Dated: October 14, 2018)

Transcriptional repression may cause transcriptional noise by a competition between repressor and RNA polymerase binding. Although promoter activity is often governed by a single limiting step, we argue here that the size of the noise strongly depends on whether this step is the initial equilibrium binding or one of the subsequent uni-directional steps. Overall, we show that non-equilibrium steps of transcription initiation systematically increase the cell to cell heterogeneity in bacterial populations. In particular, this allows also weak promoters to give substantial transcriptional noise.

I. INTRODUCTION

Protein production in living cells is the result of the combined dynamics of transcription and translation, through the activity of first RNA polymerase (RNAP) that synthesizes messenger RNA (mRNA), and subsequently the ribosomes that translate the information on mRNA to proteins. Because each mRNA typically are translated many times [1], the fluctuations in protein number are sensitive to fluctuations in the number of produced mRNA [2, 3]. Therefore there have been substantial interest in determining the noise in this number [4–7]. This noise is primarily governed by the stochastic dynamics of RNAP around the promoters, which are the regions on the DNA that direct initiation of the transcription process.

With recent availability of the technology for counting individual mRNAs in *E. coli* cells [4–7], it has become feasible to quantify the interplay between noise in gene expression and dynamics around the promoter. The degree of cell-to-cell variability in the number of a given mRNA is often quantified by the Fano factor, the ratio between the variance and the mean. The Fano factor exceeds one when the transcription is bursty. Such transcription burstiness can be obtained from a model where a gene switches between an “on-state” with high promoter activity and an “off-state” with low activity [4, 6–10]. In this simple scenario, Fano factor gives the estimate of the number of transcripts produced per “on-state”, and such a scenario can be realized by different molecular mechanisms.

Transcriptional regulators influence RNA polymerase (RNAP) access to promoters, and may cause alternating periods of low and high promoter activity, depending on the presence or absence of the regulator near the promoter (Fig. 1). When the repressor is the source of the burstiness, the measurements of the Fano factor for mRNA levels may allow for quantification of the relative sizes of on-rates of transcriptional repressors and on-rates of RNAP [9]. A recent study [10] reported Fano factors

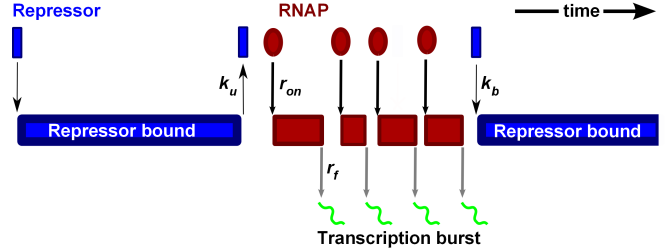


FIG. 1. Illustration of the competition between a simple transcriptional repressor (blue) and the RNA polymerase (red) in terms of the time intervals they occlude the promoter. Notice that a bound RNAP takes time to initiate transcription. It is only when the promoter is open, that there is a direct competition for the available space. The probability that the repressor wins this competition is $k_b/(k_b + r_{on})$ where r_{on} is the effective on-rate of the RNAP (see Fig. 2) and k_b is the binding rate of the repressor. The number of times the RNAP binds before the repressor rebinds is given by r_{on}/k_b .

in the presence of a transcriptional repressor. The measured dependence of noise on repressor concentration was reproduced by using a one-step model for transcription initiation, assuming that RNAP binding to the promoter sequence is the rate limiting step.

However, transcription initiation in *Escherichia coli* involves at least three steps: closed complex, open complex and elongation initiation [11, 12] (see Fig. 2) of which the two later steps are often limiting [11, 13–15]. Measuring the distributions of time intervals between two subsequent transcription events directly demonstrated that the tetA promoter has at least two limiting steps [16]. In cases where promoter activity is limited by later steps of the initiation process, the RNAP is bound to the promoter for a longer period. This inhibits the access for subsequent RNAPs as well as for transcription factors in the occluded region [17] as indicated by the red squares in Fig. 1. In fact ref. [17] studied a synthetic model system where the time RNAP spends on a promoter allowed a four fold repression of a partly overlapping promoter.

Here we analyze how mutual exclusion between transcription factors and RNAP influences the noise level. By taking the multi-step transcription initiation explic-

* mitarai@nbi.dk

† sneppen@nbi.dk

itly into account, our study emphasizes that although the activity of a promoter may be limited by a single bottleneck process, it does matter whether this limiting process is early or late in the transcription initiation process.

II. MODEL

Figure 2 illustrates the interplay between a simple transcriptional repressor, acting solely by promoter occlusion, and the activity of the promoter it regulates. The transcription factor binds to the promoter with a rate k_b when it is free, and unbind with a rate k_u . We assume the McClure three-step promoter model [11, 12] for the transcription initiation. The RNAP binds to the free promoter with a rate r_1 to form a closed complex. Subsequently it can unbind with a rate r_{-1} or form an open complex with a rate r_2 . The latter step is a non-equilibrium step, followed by a subsequent elongation initiation with a rate r_3 .

If there is no transcriptional repression, the total time between subsequent promoter initiations can now be obtained by adding together the times for the individual steps in the initiation process. This is illustrated in Fig. 2, where this total time $1/r$ is given as the sum of an effective on-time $1/r_{on} = 1/r_1 + (1/r_1) \cdot (r_{-1}/r_2)$, and the time needed for the subsequent step $1/r_f = 1/r_2 + 1/r_3$. Noticeably this sum rule incorporates all the three standard step of the McClure promoter model, with the additional caveat that the reversible binding step takes some additional time because the RNAP may bind and unbind several times before the irreversible open complex is formed. The total time between two transcription initiations is accordingly

$$\frac{1}{r} = \frac{1}{r_{on}} + \frac{1}{r_f} \quad (1)$$

where the 0.5-1 seconds time interval it take the RNAP to move away from the promoter after transcription initiation for simplicity is included in $1/r_f$. Therefore, a promoter that is limited by a small elongation initiation rate r_f can have an “on-rate” r_{on} which is much higher than its overall initiation rate $r = r_{on} \cdot r_f / (r_{on} + r_f)$ [18].

It should be noted that such multiple sequential steps in promoter initiation can reduce the Fano factor below one, if each step takes a similar time scale [8]. Obviously the process will be well-approximated by a single Poisson process if one of the steps is the rate limiting, which gives the Fano factor one. This is the largest Fano factor that the system with the sequential reaction steps can achieve.

Repressors make the reaction steps to branch out to a repressed state, which allows Fano factor to exceed one. In Fig 2, this branching happens around the “ f ” state, with the left branch representing the repressed state (“ T ” state). Noticeably, a repressor that exclusively acts through promoter occlusion only interferes with the on-rate r_{on} [9]. In other word, when the RNAP is already on the promoter, then such a repressor cannot access the

initiation complex and influence the subsequent RNAP activity. This gives the average initiation time interval under repressor $1/r_{repressed} = (1 + 1/K) \cdot (1/r_{on}) + 1/r_f$ (Fig. 2), where the dissociation constant of the repressor $K = k_u/k_b$ quantifies the binding strength of the repressor. The average mRNA number $\langle m \rangle$ is then given by [9]

$$\langle m \rangle = \frac{r_{repressed}}{\gamma} = \frac{r_{on}/\gamma}{1 + R + 1/K}, \quad (2)$$

where the aspect ratio $R = r_{on}/r_f$ characterizes the promoter architecture [18], and γ is the mRNA degradation rate.

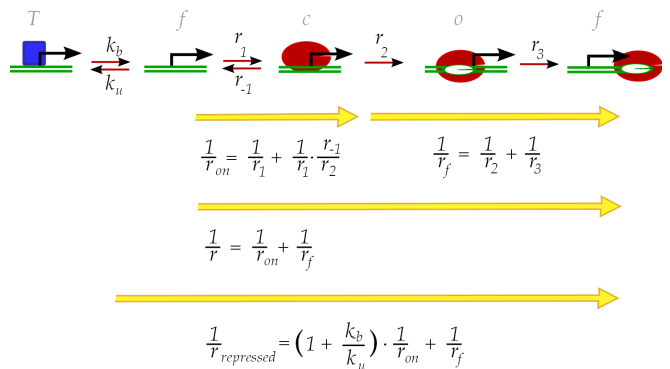


FIG. 2. Three-step promoter model of [11] exposed to a repressor. The appropriate states is marked T , f , c and o , and the figure illustrate how this can be simplified to a process that focuses on the difference between the time $1/r_{on}$ of the RNA polymerase association and the time consumed by subsequent steps. In vitro data for LacUV5 is $r_1/r_{-1} = 0.16[\text{RNAP}]/nM$ $r_2 = 0.095/\text{sec}$, $r_3 = 2/\text{sec}$ [13] where $[\text{RNAP}]$ is free RNA polymerase concentration.

The described reaction scheme (Fig. 2) provides a stochastic mRNA production process. Combined with the mRNA degradation at a constant rate γ , the variance of mRNA number in the steady state, $\sigma^2 = \langle m^2 \rangle - \langle m \rangle^2$, can be calculated by using the master equations. We performed the calculation for both the full three-step initiation model and the effective two-step initiation model described by the irreversible binding with r_{on} and subsequent elongation with a rate r_f [9]. The detail of the derivation is given in appendix A. We focus on the Fano factor $\nu = \sigma^2/\langle m \rangle$ as a measure of the cell to cell heterogeneity, which should be one if the mRNA production is a single step Poisson process.

III. RESULTS

The Fano factor for the effective two-step initiation model with repression, eq. (A2), becomes

$$\nu \equiv \frac{\sigma^2}{\langle m \rangle} \approx 1 + \frac{(r_{on}/k_b) - R \cdot K \cdot (1 + K)}{[1 + K(1 + R)]^2}. \quad (3)$$

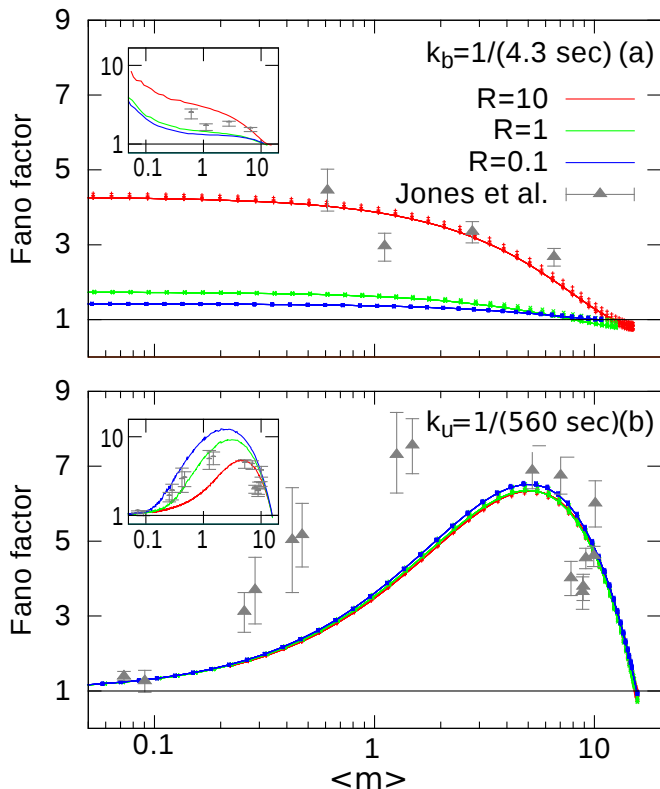


FIG. 3. Fano factor as a function of mRNA number $\langle m \rangle$ with $r/\gamma = 15.7$, $\gamma = \ln(2)/(117 \text{ sec})$ [19] and $R = 10, 1$, and 0.1 . Solid lines are for the two-step model (A2), while symbols are obtained by three-step model (A1) with combinations of r_1 , r_{-1} , r_2 , and r_3 corresponding to the used R and r . Symbols with error-bars are the corresponding experimental data from Fig. 3 in Jones *et al.* [10]. Insets show the Fano factor vs. $\langle m \rangle$ where the repressor number fluctuation is taken into account by simulating the stochastic production of repressor mRNA and protein, which makes k_b a stochastic variable. The detail of the simulation is given in Appendix B. (a) Assuming 9.8 tetramers per cell we set $k_b = 1/(4.3 \text{ sec})$. k_u is varied to change $\langle m \rangle$. Inset: Effect of cell-to-cell variation of k_b due to stochastic repressor production, with 9.8 tetramers per cell on average. (b) $k_u = 1/(560 \text{ sec})$ from [20] and k_b is varied to change $\langle m \rangle$. Inset: Effect of cell-to-cell variation of k_b , where the average repressor number is controlled through the transcription rate of the repressor mRNA.

when mRNA degradation rate (typically $\sim 1/(3 \text{ min})$ [21]) is much smaller than the repressor binding rate as well as the RNAP elongation rate ($\gamma \ll k_b$ and $\gamma \ll r_f$).

The importance of the on-rate r_{on} for the cell to cell variability becomes evident when we consider the substantially repressed genes, or genes where the concentration dependent on-rate of the repressor k_b is much higher than the off rate k_u , i.e., $K \rightarrow 0$. In this case, we have

$$\nu \approx 1 + \frac{r_{on}}{k_b}. \quad (4)$$

The increase of ν with r_{on}/k_b reflects the number of transcription initiations between each repressor binding event

[9]. The difference of eq. (4) from the simple promoter model [6, 10] is that noise can be large for a weak promoter in case its low basal activity is caused by limiting later steps in the transcription initiation (e.g. the lac promoter).

Experimentally, the noise is typically measured as a function of the average mRNA number $\langle m \rangle$ [6, 7, 10]. The average mRNA number can be controlled by either changing the repressor binding strength to the promoter (typically by altering the binding site sequence on the DNA), or by changing the concentration of the repressor. The former corresponds to changing k_u at a fixed k_b , while the latter is the other way around.

For a fixed repressor concentration (constant k_b), from (2) we can express k_u as a function of $\langle m \rangle$. Replacing k_u in the Fano factor, one get

$$\nu \approx 1 + \frac{r_{on}}{k_b^*} \cdot \left(1 - \frac{\langle m \rangle}{m_{max}}\right)^2 \quad (5)$$

with $m_{max} \equiv r/\gamma$, where the approximation ignores a reduction term in Fano factor, which is small when $\langle m \rangle < m_{max}$, see eq. (3).

The prefactor is governed by the γ -corrected association rate $k_b^* \approx k_b + \gamma(R+1)(1 - \frac{\langle m \rangle}{m_{max}}) \sim k_b$. This means that ν decreases monotonically with $\langle m \rangle$ when the change is caused by increased k_u (by operator mutations).

As an illustration we now consider the substantial Fano factors that was measured on the Lac system by [10]. A one-step model ($R \ll 1$) would require k_b values that are much smaller than the overall initiation rate r ($\sim 1/(11 \text{ sec})$) for the measured Lac system [10, 19]) to have a Fano factor substantially larger than 1, because $r_{on} \approx r$ when $R \ll 1$. Indeed [10] uses the binding rate for one Lac tetramer to be one per 6.3 minutes to fit the measured ν with a one-step model. However, this rate may be too slow given that the association rate of one Lac-dimer is estimated to be about $1/3.5 \text{ min}$ [22], and is found to bind 5 fold slower than a Lac-tetramer [23, 24], suggesting an association rate per tetramer of $1/42 \text{ sec}$ in an *E. coli* cell.

The multi-step models can give high Fano factors at much higher values of k_b . Spassky *et al.* [13] measured that open complex formation takes $1/r_2 \sim 10 \text{ sec}$ for the lacUV5 promoter in vitro, which combined with $r \sim 11 \text{ sec}$ suggest that this later step is rate limiting and that $R \gg 1$. Our analysis assuming $R = 10$ and on-rate of a single Lac-tetramer of $1/42 \text{ sec}$ gives the Fano factors of ~ 4 with ~ 10 tetramers per cell, consistent with the experimental data by Jones *et al.* [10] (Fig.3a).

Consider now a given operator (constant k_u) and change $\langle m \rangle$ by regulating the repressor concentration (k_b). The Fano factor in this case is

$$\nu \approx 1 + \frac{\gamma}{k_u^*} \cdot \langle m \rangle \cdot \left(1 - \frac{\langle m \rangle}{m_{max}}\right), \quad (6)$$

with the γ -corrected dissociation rate $k_u^* \approx k_u + \gamma \cdot \langle m \rangle / m_{max} \approx k_u$. Eq. (6) is non-monotonic, with largest

ν at half maximum expression $\langle m \rangle \sim m_{max}/2$ (Fig. 3b). The functional dependence of ν with $\langle m \rangle$ in Eq. (6) does not depend on R , but the interpretation of the underlying dynamics does. Noticeably, to obtain a given repression level m/m_{max} for a promoter with $R \gg 1$ the repressor needs a factor $(1 + R)$ stronger binding than naively expected. This reflects that the repressor has to act in the reduced time where the promoter is not occupied by RNA polymerase [9], see Fig. 1. A corollary of this interplay is that estimates of repressor binding energies from promoter activities also rely on the non-equilibrium aspects of the RNAP-promoter dynamics.

Finally one may notice that the fit in Fig. 3b underestimates the measured noise level. Part of this is attributed to the fact that we use a rate k_b that is the same for all cells at a given repression level. The Lac-tetramer in fact comes at small numbers [25], even at the highly repressed state (to the left of Fig. 3b), and the cell-to-cell fluctuations can be substantial. This will add to the Fano-factor and in particular increase the variation of mRNA for intermediate repression levels, and make the maximum Fano-factor to be reached substantially below the $\langle m \rangle \sim m_{max}/2$ value predicted by eq. 6.

We simulated this effect by considering stochastic production and degradation of the repressor (Fig. 3b inset). The system is more sensitive to this fluctuation for smaller R , because the repressor is more effective (see eq. 2). In the simulation, we set the parameter so that one repressor is produced per one repressor mRNA. The effect will be naturally larger if more than four LacI monomers are produced per mRNA. Also the effect will be stronger when the chromosome copy number is larger than one, because fluctuations of repressor act simultaneously on each gene copy.

For Fig. 3a, the fluctuation of repressor number also increase the Fano factor (Fig. 3a inset), but a larger R shows a larger Fano factor for the same $\langle m \rangle$. This is because to achieve the same $\langle m \rangle$, k_u needs to be smaller for larger R , which makes the dynamics more bursty and sensitive to the repressor number fluctuation.

IV. DISCUSSION

The above analyses only apply to repressors that act by simple occlusion, and do not affect the post binding steps of transcription initiation. In case a transcriptional repressor acts by stalling the isomerization step [14, 15], it does not occlude the RNAP binding site and the noise should scale with r as suggested by the $R \ll 1$ limit [6]. In case the transcriptional regulator is an activator, it may act through modification of r_1 , r_{-1} , r_2 or r_3 [14] but will not occlude the promoter, and we therefore expect the burstiness to be reproduced by considering an overall initiation rate modulation as implied in the formalism of [6].

This short paper aimed to clarify the interplay between time-scales of transcription initiation, and time-

scales of transcriptional repressors in prokaryotes. As an added benefit, the formalism propose to use measurements of the Fano factor as a tool to determine the ratio of two competing rates (eq. (4)). By exposing for example a promoter with large r_{on} to different repressors, one may compare repressor dynamics. Conversely, by exposing different promoters to the same repressor/operator combination, one may quantify their relative on-rates for RNAP. To be truly useful, such an experimental design should preferentially use a repressor which exhibits minimal noise, as one thereby reduce the extrinsic noise.

Finally, although Fano factors in principle are robust to having multiple copies of a given promoter in the E.coli cell, then one should be aware that failure in detecting all mRNA will make the experimentally measured Fano factor systematically smaller than the real one,

$$\nu_{measured} = 1 + p \cdot (\nu - 1) \quad (7)$$

where p is the probability for observing a mRNA in the cell (detail in appendix C). For instance, the procedures based on counting individual spots tend to underestimate the number of mRNA molecules [26]; the highest value of mRNA per cell reported in ref. [5], which uses the counting method, is less than 10, while ref. [6] that uses the total intensity to estimate the mRNA number reports ~ 50 mRNAs per cell. Thus, if p is say 0.2, then a real burst size of $\nu \sim 9$ would only be detected as $\nu_{measured} \sim 2.6$. Therefore a measured Fano factor should be corrected by the estimated likelihood for identifying individual mRNAs in the cell.

Using ν as a experimental tool to learn about promoter dynamics would further be facilitated by reporter mRNAs with relatively large lifetimes (small γ). Central in such an analysis is to realize that transcriptional noise is primarily sensitive to the first steps of the transcription initiation process (Fig. 3), and thereby cell to cell variations becomes sensitive to the limiting process of individual promoters.

Appendix A: Derivation of the Fano factor

We summarize the derivation of the Fano factor for the model described in Fig. 2. In the three-step transcription initiation model, the promoter can be in one of the following four states: free (f), RNAP forming a closed complex (c), RNAP forming an open complex (o), and bound by the transcriptional repressor (T). In this model repressor binding does not influence open complex formation or the rate of elongation initiation. We denote the probability for the promoter to be in the state α and having m mRNAs at time t to be $P_m^\alpha(t)$, where α can be f , c , o , or T . Assuming that a mRNA is produced at the moment the RNAP elongates (this ignores the deterministic clearance time), we have the following master

equations:

$$\begin{aligned}
\dot{P}_m^f(t) &= r_3 P_{m-1}^o(t) + k_u P_m^T(t) + r_{-1} P_m^c(t) - (r_1 + k_b) P_m^f(t) \\
&\quad + \gamma \left[(m+1) P_{m+1}^f(t) - m P_m^f(t) \right], \\
\dot{P}_m^c(t) &= r_1 P_m^f(t) - (r_{-1} + r_2) P_m^c(t) \\
&\quad + \gamma \left[(m+1) P_{m+1}^c(t) - m P_m^c(t) \right], \\
\dot{P}_m^o(t) &= r_2 P_m^c(t) - r_3 P_m^o(t) \\
&\quad + \gamma \left[(m+1) P_{m+1}^o(t) - m P_m^o(t) \right], \\
\dot{P}_m^T(t) &= k_b P_m^f(t) - k_u P_m^T(t) \\
&\quad + \gamma \left[(m+1) P_{m+1}^T(t) - m P_m^T(t) \right].
\end{aligned}$$

The probability to have m mRNAs in the system at time t irrespective of the promoter/operator state is given by $P_m(t) \equiv P_m^f(t) + P_m^c(t) + P_m^o(t) + P_m^T(t)$. The Fano factor $\nu = (\langle m^2 \rangle - \langle m \rangle^2) / \langle m \rangle$ was obtained by calculating $\langle m \rangle = \sum_{m=0}^{\infty} m P_m$ and $\langle m^2 \rangle = \sum_{m=0}^{\infty} m^2 P_m$ in the steady state using the generating function method [27]. The resulting Fano factor for the three-step model is given by

$$\nu_{3\text{-step}} = 1 + \frac{\frac{r_{on}}{k_b} - K(1 + K^*) \left(\frac{r_{on}}{r_3} + \frac{r_{on}^2}{r_1 r_2} + \frac{\gamma r_{on}^2}{r_1 r_2 r_3} \right) - \frac{r_{on}^2}{r_2 r_3} K K^*}{\left[K^* \left(R + \frac{\gamma r_{on}}{r_2 r_3} \right) + \left(1 + \frac{\gamma}{r_3} \right) (1 + K^*) \left(1 + \frac{\gamma r_{on}}{r_1 r_2} \right) \right] \cdot [1 + K \cdot (1 + R)]}. \quad (\text{A1})$$

with $K^* \equiv K + \gamma/k_b$ and the on-rate $r_{on} = r_1 \cdot r_2 / (r_{-1} + r_2)$ that is modulated from the rate r_1 because the RNAP may unbind from the promoter.

The Fano factor for the effective two-step initiation model (RNAP binding and elongation initiation) can also

be obtained similarly, or by taking $r_2 \rightarrow \infty$ limit of eq. (A1) noting that $r_{on} \rightarrow r_1$ and $r_f \rightarrow r_3$ in this limit. The full expression of the Fano factor for the effective two-step model is given by

$$\nu_{2\text{-step}} = 1 + \frac{(r_{on}/k_b) - R \cdot K \cdot (1 + K^*)}{[1 + K^*(1 + R) + (\gamma/r_f)(1 + K^*)] \cdot [1 + K \cdot (1 + R)]}. \quad (\text{A2})$$

Appendix B: Stochastic fluctuation of the repressor number

We assume that the repressor mRNA is transcribed at a constant rate α and degraded at a rate Γ_m per mRNA. Each mRNA is translated at a rate β to produce a repressor and the repressor is degraded at a rate Γ_p per repressor, as parametrized in [2]. For simplicity, we assume that a produced repressor corresponds to a LacI tetramer. We employ the two-step model in Fig. 2 for the promoter dynamics, with making the repressor binding rate dependent on the number of repressor molecules N_r as $k_b = k_0 \cdot N_r$, where $k_0 = 1/(42 \text{ sec})$ is the single repressor binding rate. For all the simulations, we assumed $\Gamma_m = \ln(2)/(120 \text{ sec})$, $\Gamma_p = \ln(2)/(40 \text{ min})$, and

$\beta = \Gamma_m$, i.e., one repressor tetramer is produced per mRNA on average. For Fig. 3(a) inset, α is set to be $9.8 \cdot \Gamma_m \cdot \Gamma_p / \beta$ to have 9.8 repressors (tetramers) on average, while Fig. 3(b) inset, α is changed to control $\langle m \rangle$. The reactions were simulated by Gillespie method [28], and averages were calculated from the data.

Appendix C: Effect of limited detection on the measured Fano factor

Suppose when we make the observation, each mRNA can be observed with a constant probability p . When the probability to have m mRNA is P_m , then the probability

$Q(n)$ to observe n mRNAs is

$$Q(n) = \sum_{m=0}^{\infty} \frac{m!}{n!(m-n)!} p^n (1-p)^{m-n} P_m \Theta(m-n), \quad (\text{C1})$$

where $\Theta(x)$ is the Heaviside step function. This gives

$$\langle n \rangle = \sum_{n=0}^{\infty} n Q(n) = p \langle m \rangle,$$

and

$$\langle n^2 \rangle = p^2 \langle m(m-1) \rangle + p \langle m \rangle.$$

This results in the measured Fano factor to be

$$\begin{aligned} \nu_{\text{measured}} &= \frac{\langle n^2 \rangle - \langle n \rangle^2}{\langle n \rangle} = p \frac{\langle m^2 \rangle - \langle m \rangle^2}{\langle m \rangle} + (1-p) \\ &= 1 + p \cdot (\nu - 1), \end{aligned} \quad (\text{C2})$$

where ν is the actual value of the Fano factor.

ACKNOWLEDGMENTS

We thank for support from the Danish National Research Foundation through the Center for Models of Life.

-
- [1] H. Bremer and P. P. Dennis, (1996).
 - [2] N. Friedman, L. Cai, and X. S. Xie, *Physical review letters* **97**, 168302 (2006).
 - [3] J. Yu, J. Xiao, X. Ren, K. Lao, and X. S. Xie, *Science* **311**, 1600 (2006).
 - [4] I. Golding, J. Paulsson, S. M. Zawilski, and E. C. Cox, *Cell* **123**, 1025 (2005).
 - [5] Y. Taniguchi, P. J. Choi, G.-W. Li, H. Chen, M. Babu, J. Hearn, A. Emili, and X. S. Xie, *Science* **329**, 533 (2010).
 - [6] L.-h. So, A. Ghosh, C. Zong, L. A. Sepúlveda, R. Segev, and I. Golding, *Nature genetics* **43**, 554 (2011).
 - [7] A. Sanchez and I. Golding, *Science* **342**, 1188 (2013).
 - [8] N. Mitarai, I. B. Dodd, M. T. Crooks, and K. Sneppen, *PLoS computational biology* **4**, e1000109 (2008).
 - [9] H. Nakanishi, N. Mitarai, and K. Sneppen, *Biophysical journal* **95**, 4228 (2008).
 - [10] D. L. Jones, R. C. Brewster, and R. Phillips, *Science* **346**, 1533 (2014).
 - [11] W. R. McClure, *Proceedings of the National Academy of Sciences* **77**, 5634 (1980).
 - [12] D. K. Hawley and W. R. McClure, *Proceedings of the National Academy of Sciences* **77**, 6381 (1980).
 - [13] A. Spassky, K. Kirkegaard, and H. Buc, *Biochemistry* **24**, 2723 (1985).
 - [14] S. Roy, S. Garges, and S. Adhya, *Journal of Biological Chemistry* **273**, 14059 (1998).
 - [15] S. Roy, S. Semsey, M. Liu, G. N. Gussin, and S. Adhya, *Journal of molecular biology* **344**, 609 (2004).
 - [16] A.-B. Muthukrishnan, M. Kandhavelu, J. Lloyd-Price, F. Kudasov, S. Chowdhury, O. Yli-Harja, and A. S. Ribeiro, *Nucleic acids research* **40**, 8472 (2012).
 - [17] K. M. Bendtsen, J. Erdőssy, Z. Csiszovszki, S. L. Svenningsen, K. Sneppen, S. Krishna, and S. Semsey, *Nucleic acids research* **39**, 6879 (2011).
 - [18] K. Sneppen, I. B. Dodd, K. E. Shearwin, A. C. Palmer, R. A. Schubert, B. P. Callen, and J. B. Egan, *Journal of molecular biology* **346**, 399 (2005).
 - [19] C. Petersen, *Molecular and General Genetics MGG* **209**, 179 (1987).
 - [20] P. Hammar, M. Walldén, D. Fange, F. Persson, Ö. Baltekin, G. Ullman, P. Leroy, and J. Elf, *Nature genetics* **46**, 405 (2014).
 - [21] S. Pedersen, S. Reeh, and J. D. Friesen, *Molecular and General Genetics MGG* **166**, 329 (1978).
 - [22] P. Hammar, P. Leroy, A. Mahmutovic, E. G. Marklund, O. G. Berg, and J. Elf, *Science* **336**, 1595 (2012).
 - [23] M. Hsieh and M. Brenowitz, *Journal of Biological Chemistry* **272**, 22092 (1997).
 - [24] S. Oehler, E. R. Eismann, H. Krämer, and B. Müller-Hill, *The EMBO journal* **9**, 973 (1990).
 - [25] S. Semsey, L. Jauffred, Z. Csiszovszki, J. Erdőssy, V. Stéger, S. Hansen, and S. Krishna, *Nucleic acids research* **41**, 6381 (2013).
 - [26] S. O. Skinner, L. A. Sepúlveda, H. Xu, and I. Golding, *Nature protocols* **8**, 1100 (2013).
 - [27] N. G. Van Kampen, *Stochastic processes in physics and chemistry*, Vol. 1 (Elsevier, 1992).
 - [28] D. T. Gillespie, *The journal of physical chemistry* **81**, 2340 (1977).